

# RSC Advances



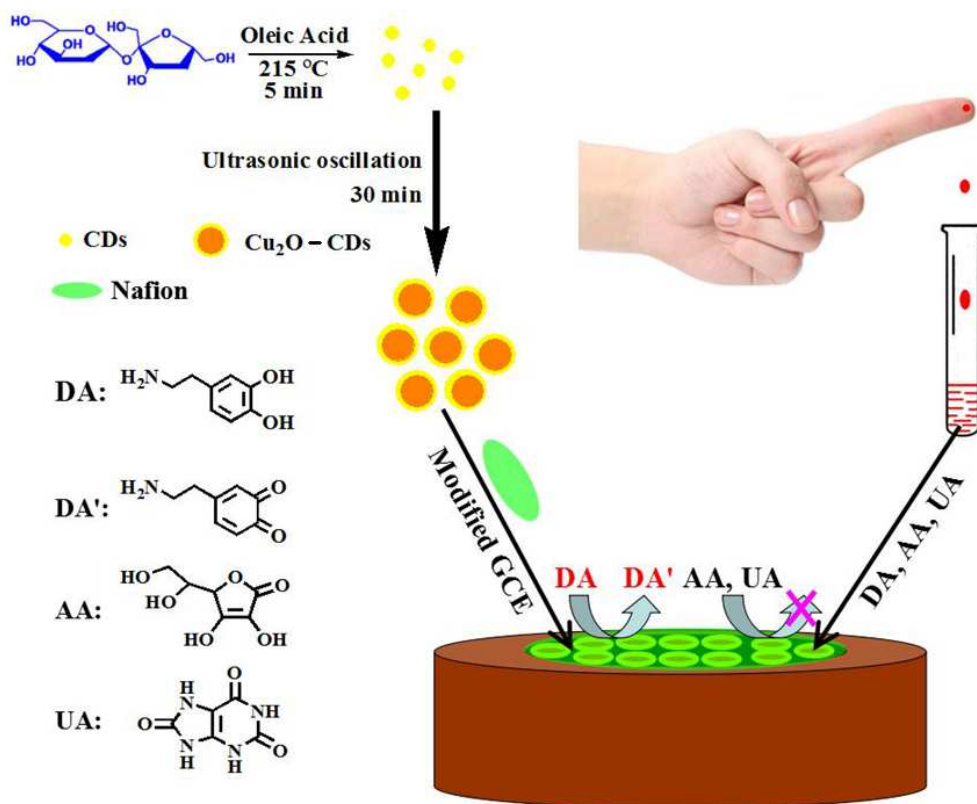
This is an *Accepted Manuscript*, which has been through the Royal Society of Chemistry peer review process and has been accepted for publication.

*Accepted Manuscripts* are published online shortly after acceptance, before technical editing, formatting and proof reading. Using this free service, authors can make their results available to the community, in citable form, before we publish the edited article. This *Accepted Manuscript* will be replaced by the edited, formatted and paginated article as soon as this is available.

You can find more information about *Accepted Manuscripts* in the [Information for Authors](#).

Please note that technical editing may introduce minor changes to the text and/or graphics, which may alter content. The journal's standard [Terms & Conditions](#) and the [Ethical guidelines](#) still apply. In no event shall the Royal Society of Chemistry be held responsible for any errors or omissions in this *Accepted Manuscript* or any consequences arising from the use of any information it contains.

## Graphical abstract



**A high performance electrochemical biosensor based on Cu<sub>2</sub>O-carbon dots for selective and sensitive determination of dopamine in human serum**

Qitong Huang <sup>a\*</sup>, Xiaofeng Lin <sup>c\*</sup>, Changqing Lin <sup>a</sup>, Yong Zhang <sup>a,b</sup>, Shirong Hu <sup>c</sup>, Chan Wei <sup>c</sup>

<sup>a</sup> Department of Food and Biological Engineering, Zhangzhou Institute of Technology,  
Zhangzhou, 363000, P.R. China

<sup>b</sup> Research of Environmental Science, Xiamen University,  
Xiamen, 361005, PR China.

<sup>c</sup> College of Chemistry and Environment, Minnan Normal University,  
Zhangzhou, 363000, PR China.

---

\*Corresponding author: Tel: +86 596-2660090. Fax: + 86 596-2660090.

E-mail address: hqtblue@163.com (Q. Huang).

E-mail address: Lxf0596@163.com (X. Lin).

**Abstract:** A green and facile method was developed by synthesizing a cuprous oxide-carbon dots/Nafion ( $\text{Cu}_2\text{O}$ -CDs/NF) composite film for highly sensitive and reliable determination of dopamine (DA). The  $\text{Cu}_2\text{O}$  nanoparticle could improve the conductivity of the electrode, while the CDs with carboxyl groups and the NF with sulfo groups could attract cations via the ion-exchange model and exclude anions by the electrostatic action. The proposed biosensor exhibited low detection limit of 1.1 nM with wide linear range of 0.05  $\mu\text{M}$  - 45.0  $\mu\text{M}$  and acquired excellent sensitivity and selectivity for DA. Furthermore, the  $\text{Cu}_2\text{O}$ -CDs/NF/GCE also was applied to determine DA in human serum with satisfactory results and showed a good activity for more than two month.

**Keywords:** Cuprous oxide; carbon dots; dopamine; nafion; electrochemistry biosensor

## 1. Introduction

In recent years, nanomaterials have made an important impact on diverse science, engineering, and commercial sectors due to their high catalysis, low cost, and good stability.<sup>1-5</sup> Cuprous oxide ( $\text{Cu}_2\text{O}$ ), as a p-type semiconductor, has drawn intense interest in the past decade, not only for its unique properties but also for its applications in various fields such as gas sensors,<sup>6</sup> solar cells,<sup>7</sup> lithium ion batteries,<sup>8</sup> catalysis<sup>9</sup> and so on. As a star-rated material,  $\text{Cu}_2\text{O}$  nanomaterials have been continually used as an ideal material for fabricating electrochemical biosensors due to their ultrahigh electrocatalysis capacity and surface area effect in biosensing analysis.<sup>10</sup> Due to the 'zero-dimensional' feature, carbon dots (CDs) had become one of the hottest materials in many fields, such as physics, chemistry, biological imaging and electronics since their discovery in 2004.<sup>11-13</sup> The advantages of low toxicity, excellent biocompatibility, high chemical stability and remarkable conductivity, which make it as a good electrode material to construct various electrochemical platforms.<sup>14</sup> What's more, the CDs also can be used as reducing agents,<sup>15,16</sup> which can directly reduce copper hydroxide to form  $\text{Cu}_2\text{O}$ -CDs without adding other reducers or stabilizers.

Belonging to the family of excitatory chemical neurotransmitters, dopamine (DA) acts as one of the most significant catecholamines, which plays a pivotal role in the function of human metabolism, cardiovascular, renal, central nervous and hormonal systems.<sup>17-20</sup> As known, electrochemical biosensors have attracted tremendous efforts recently as a novel analytical tool due to its selectivity, sensitivity, simplicity and rapid response time.<sup>21-24</sup> Due to DA's electrochemical activity, DA detection is always attracting the intense interest in electroanalysis, such as gold nanoparticles-reduced graphene oxide sheets-indium tin oxide-coated glass (AuNPs-rGOS-ITO),<sup>17</sup> copper nanoparticles-multi-walled carbon nano-tubes/glassy carbon electrode (Cu-MWCNT/GCE),<sup>18</sup>  $\text{WO}_3$  nanoparticles,<sup>19</sup> and so on. In this work, a green and economical composite of  $\text{Cu}_2\text{O}$ -CDs/Nafion (NF) composite was utilized to construct a novel dopamine (DA) biosensor. To the best of our knowledge, electrochemical detection of DA utilizing the  $\text{Cu}_2\text{O}$ -CDs/NF based hybrid film has not been published. The  $\text{Cu}_2\text{O}$  nanoparticle could increase surface area of the GCE, the CDs had carboxyl groups and the NF had sulfo groups, they could attract cations via the ion-exchange model and exclude anions by the electrostatic action, which could improve the selectivity in the detection of DA.<sup>16,25</sup> Therefore, the  $\text{Cu}_2\text{O}$ -CDs/NF composite provided an excellent platform for sensitive, selective and reliable determination of DA. In addition, the modified electrode was applied to detect DA content in the human serum with satisfactory results.

## 2. Experimental

### 2.1. Reagents and instrumentation

Glucose, ethanol, ascorbic acid, uric acid and dopamine were purchased from Sinopharm Chemical Reagent Co., Ltd. (Shanghai, China). Sodium hydroxide, oleic acid and copper nitrate were purchased from Xilong Chemical Co., Ltd. (Guangdong, China). Nafion was purchased from Sigma-Aldrich Chem. Co. (USA) (5 wt% in mixture of lower aliphatic alcohols and H<sub>2</sub>O). All the solutions were prepared with deionized water (18.2 MΩ).

All of electrochemical experiments were performed with CHI 660E electrochemical workstation (Shanghai Chenhua Instruments Co., China). A conventional three-electrode system was used in all electrochemical experiments, which consist a platinum wire auxiliary electrode, a Ag|AgCl (saturated KCl) reference electrode and a bare or modified GCE as working electrode, which. Scanning electron microscope (SEM) imaging was performed on a S-4800 electron microscope (Hitachi, Ltd., Japan). TEM images were measured using a JEM-100CX electron microscope from JEOL Ltd (Aichi Kariya, Japan). The surface morphology of the Cu<sub>2</sub>O-CDs/NF film was characterized using atomic force microscopy (AFM, CSPM5500, China). All experiments were carried out at room temperature.

### 2.2. Synthesis of Cu<sub>2</sub>O-CDs composite and Cu<sub>2</sub>O-CDs/NF composite film

The synthesis of CDs were synthesized follow previous report.<sup>26</sup> Cu<sub>2</sub>O-CDs composite were synthesized by adding 100 μL aqueous solution of Cu(NO<sub>3</sub>)<sub>2</sub> (1.0 mol L<sup>-1</sup>) was added to 200 μL aqueous solution of NaOH (1.0 mol L<sup>-1</sup>). After 20 min, 100 μL CDs solution (8.0 mg mL<sup>-1</sup>) was added to the above solution. Then the mixed solution was kept at 90 °C for 30 min to yield a stable purple solution of Cu<sub>2</sub>O-CDs. After that, the Cu<sub>2</sub>O-CDs/NF composite film was carried out: 50.0 μL NF was added in 450.0 μL ethanol to forming homogeneous solution. Then 100.0 μL Cu<sub>2</sub>O-CDs solution was added in Nafion ethanol solution with vigorous ultrasonication.

## 3. Results and discussion

### 3.1. Characterization of CDs, Cu<sub>2</sub>O-CDs and Cu<sub>2</sub>O-CDs/NF/GCE

The TEM image of the CDs was shown in the **Fig. 1A**. It can be seen that the sizes of CDs were ranging from 1.0 nm to 5.0 nm. The Cu<sub>2</sub>O-CDs (**Fig. 1B**) was characterized by SEM with the sizes ranging from 30.0 nm to 70.0 nm. The UV-Vis spectrum of CDs and Cu<sub>2</sub>O-CDs were shown in the **Fig. 1C**, The CDs had a strong absorption band appear at 281 nm and. As known the absorption band of Cu<sub>2</sub>O nanocubes (<100 nm) was range from 450 nm to 490 nm.<sup>27</sup> However, the Cu<sub>2</sub>O-CDs exhibited

two characteristic absorption peaks at 284 nm and 426 nm, due to the CDs' impact, the peak of Cu<sub>2</sub>O had a blue-shift. The XRD (**Fig. 1D**) was also showed the nanocompound of Cu<sub>2</sub>O-CDs were formed. The XRD data of the three as-synthesized samples were all in good agreement with those of Cu<sub>2</sub>O (JCPDSNO.65-3288), the 5 typical peaks located at 29.70°, 36.41°, 42.25°, 61.27° and 73.54°, which were attributed to the (110), (111), (200), (220) and (311) planes of cuprous oxide, respectively. No characteristic peaks arising from Cu or CuO could be observed in the XRD patterns, indicating that the products obtained via our synthetic routes consist of only Cu<sub>2</sub>O phase. In addition, a broad peak located at 20.02° which indicated the CDs existed in the nanocompound.<sup>9,26</sup> Furthermore, 3D AFM images of the bare GCE, NF/GCE, CDs/NF/GCE and Cu<sub>2</sub>O-CDs/NF/GCE were shown in **Fig. 2**. **Fig. 2A** showed that the bare GCE was relatively flat and smooth with the average roughness of +1.22 nm, while after NF (**Fig. 2B**) and CDs/NF (**Fig. 2C**) modification, the average roughness increased to +1.73 nm and +2.51 nm, respectively. However, for Cu<sub>2</sub>O-CDs/NF/GCE, an average roughness of +10.42 nm was observed (**Fig. 2D**). From the AFM results, it was also obtained that the largest height of Cu<sub>2</sub>O-CDs/NF/GCE was determined to be 48.27 nm, which is obviously larger than the bare GCE (5.25 nm), NF (8.03 nm) and CDs/NF (12.91 nm). These results demonstrated that Cu<sub>2</sub>O-CDs/NF had been anchored on GCE and improved the surface effect of the electrode interface.

**Fig. 1**

**Fig. 2**

### 3.2. Cyclic voltammetric behavior of DA on the Cu<sub>2</sub>O-CDs/NF/GCE

**Fig. 3** showed the typical cyclic voltammograms (CVs) of DA on the bare GCE (a), NF/GCE (b) CDs-NF/GCE (c) and Cu<sub>2</sub>O-CDs/NF/GCE in 0.1 mol/L pH 7.0 PBS at the scan rate of 0.1 V s<sup>-1</sup>. Well resolved, defined and more enhanced anode current peak is observed on Cu<sub>2</sub>O-CDs/NF/GCE compared to GCE, NF/GCE, CDs-NF/GCE. The oxidation peak current intensity at Cu<sub>2</sub>O-CDs/NF/GCE was increased 3.16 times, 2.08 times, 1.88 times higher than those obtained at GCE, NF/GCE and CDs-NF/GCE, respectively. A possible reaction mechanism of Cu<sub>2</sub>O-CDs/NF/GCE with DA was discussed that the Cu<sub>2</sub>O nanoparticle could make the surface of the electrode more conductive, the CDs had carboxyl groups and NF had sulfo groups which could make it have good stability for sensitive and selective determination of DA.

**Fig. 3**

### 3.3 Effects of pH and scan rate on DA detection at Cu<sub>2</sub>O-CDs/NF/GCE

The effect of the pH of PBS on dopamine detection at Cu<sub>2</sub>O-CDs/NF/GCE was examined by CVs, and the results were shown in **Fig. 4A**. The results showed that the oxidation peak currents of DA first increased as the pH increase from 5.0 to 7.0, and then decreased as pH further increased from 7.0 to 9.0. The oxidation peak current reached a maximum at pH = 7.0.. Therefore, the pH = 7.0 was used in the experiments to achieve the highest sensitivity. At the same time, the oxidation peak potential shifted negatively with the increase of pH value, indicating that protons involved in the electrode reaction. A good linear relationship between  $E_{pa}$  and pH was established by fitting with a linear regression equation as  $E_{pa}$  (V) = -0.0574 pH + 0.722 ( $R^2 = -0.997$ ,  $n = 5$ ). The slope value of -57.4 mV/pH showed that the electron transfer was accompanied by an equal number of protons.<sup>28</sup>

In order to further investigate the electrochemical behavior of DA at the Cu<sub>2</sub>O-CDs/NF/GCE, **Fig. 4B** presents CVs of DA in 0.1M PBS (pH 7.0) at the Cu<sub>2</sub>O-CDs/NF/GCE at different scan rate. The redox peak currents increases monotonically as scan rate increases. Both of the anodic and cathodic peak currents follow a linear relationship with the scan rate in a range from 0.05 to 0.5 V s<sup>-1</sup> (**Fig. 4C**), For anodic peak currents was  $I_{pa}$  (μA) = -12.124  $\nu$  - 2.943 ( $R^2 = 0.997$ ,  $n = 5$ ). For cathodic peak current was  $I_{pc}$  (μA) = 7.983  $\nu$  - 0.771 ( $R^2 = 0.995$ ,  $n = 5$ ). This implied that the electrochemical oxidation of DA at the Cu<sub>2</sub>O-CDs/Nafion/GCE was a surface-controlled process, but not a diffusion-controlled process. In addition, the influence of scan rate on the peak potential was also investigated by CVs. As shown in the **Fig. 4D**, the anodic and cathodic peak currents peak potential followed a linear relationship with the logarithm of scan rate. The regression equations were  $E_{pa}$  (V) = 0.0442 log $\nu$  + 0.357 ( $R^2 = 0.995$ ,  $n = 5$ ) and  $E_{pc}$  (V) = -0.0291 log $\nu$  + 0.0367 ( $R^2 = 0.997$ ,  $n = 5$ ), respectively. The relationship between the potential and scan rate could be described as following equations by Laviron.<sup>29</sup>

$$E_{pa} = E^{0'} + \frac{2.3RT}{(1-\alpha)nF} \log \nu \quad (1)$$

$$E_{pc} = E^{0'} - \frac{2.3RT}{\alpha nF} \log \nu \quad (2)$$

$$\log k_s = \alpha \log(1-\alpha) + (1-\alpha) \log \alpha - \log \frac{RT}{nF\nu} - \frac{(1-\alpha)\alpha nF \Delta E_p}{2.3RT} \quad (3)$$

Where  $\alpha$  was the electron transfer coefficient,  $n$  was the number of transfer electron,  $k_s$  was the standard heterogeneous rate constant,  $R$ ,  $T$  and  $F$  had their usual significance. After making



computations:  $\alpha = 0.603$ ,  $n = 2.32$ ,  $k_s = 1.48 \text{ s}^{-1}$ . The value of  $k_s$  was bigger than some reported values,<sup>23</sup> indicating a fast electron transfer reaction on the Cu<sub>2</sub>O-CDs/NF/GCE.

#### Fig. 4

##### 3.4. Interference effect

As known that the oxidation peak potentials for ascorbic acid (AA), uric acid (UA) and DA were very close to each other on a bare GCE, hence, it was difficult to separate these compounds due to their overlapping signals.<sup>30</sup> Now, the problem could be eliminated in this study. Using the Cu<sub>2</sub>O-CDs/NF/GCE as the working electrode, The CDs had carboxyl groups and the NF had sulfo groups could prevent anionic AA and UA from reaching the electrode surface, which was in its anionic form at the working electrode surface in the pH 7.0 phosphate buffer solution, both AA (pKa = 4.10) and UA (pKa = 5.75) were negatively charged, but DA (pK = 8.89) was positively charged at physiological pH = 7.0.<sup>31</sup> As shown in **Fig. 5**, it could be concluded that the presence of AA and UA did not interfere in the DA determination.

Furthermore, other influences from common co-existing substances were also investigated. When the relative error (Er) exceeded 5 %, each matter was considered as an interfering agent. It was found that most ions and common substances at high concentration only caused negligible change: Na<sup>+</sup>, K<sup>+</sup>, NO<sub>3</sub><sup>-</sup>, Cl<sup>-</sup>, SO<sub>4</sub><sup>2-</sup> (>200 fold), Ca<sup>2+</sup>, Zn<sup>2+</sup>, (100 fold), lysine, cysteine and glucose (60 fold), The results indicated the Cu<sub>2</sub>O-CDs/NF/GCE exhibited good selectivity for DA detection.

#### Fig. 5

##### 3.5. Calibration curve

The calibration curve of DA on Cu<sub>2</sub>O-CDs/NF/GCE was investigated by differential pulse voltammetry (DPVs) (**Fig. 6A**). It was found that under optimal experimental conditions the peak current increases with DA concentration, and the oxidation peak current ( $I_{pa}$ ) has a good linear relationship with DA concentration in the range of 0.05  $\mu\text{M}$  - 45.0  $\mu\text{M}$ . As shown in **Fig. 6B**, the linear regression equation was described as  $I_{pa} (\mu\text{A}) = -0.0773 C_{DA} - 2.301$  ( $R^2 = 0.998$ ,  $n = 5$ ), giving a detection limit of 1.1 nM ( $S/N = 3$ ). The detection limit was calculated as 1.1 nM, lower than some previous reports (**Table 1**) which had been published on **RSC Advances** and other other published in 2015,<sup>19,32-39</sup> indicating that Cu<sub>2</sub>O-CDs/NF/GCE had good sensitivity. The stability of the Cu<sub>2</sub>O-CDs/NF/GCE was also examined, the Cu<sub>2</sub>O-CDs/NF/GCE was put into a vacuum drying oven at

25 °C, after one week the amperometric responses 99.2% remained against its initial value, 96.5% one month later and 91.3% two months later. The intra- and inter-assay measurements had been also done, and all the experimental errors was under 2%, which indicated the reproducibility for the preparation of electrodes was satisfactory. The excellent characteristics demonstrated the feasibility of its practical application.

### Fig. 6

### Table 1

#### 3.6. Sample analysis

In order to evaluate the applicability of the proposed method to the determination of DA in real samples, the utility of the developed method was tested by determining DA in human serum (The sample preparation and adequate dilution steps as described earlier)<sup>40</sup>. The results were summarized in **Table 2**. The recovery rates of the samples ranged between 99.4% and 103.8%, which indicated that the presence of AA, UA and some other substances, such as glucose and sodium chloride did not interfere with the determination of DA. Therefore, the proposed method could be effectively used for the direct determination of DA in real samples.

### Table 2

#### 4. Conclusions

In this study, we have demonstrated a simple combustion method to prepare Cu<sub>2</sub>O-CDs with remarkable conductivity by using CDs directly reduce copper hydroxide. then it was used as working electrode for sensitive and selective determination of DA with the detection limit of 2.2 nM, which are superior to those measured for other metal oxide nanoparticles based working electrode. Due to high yield and efficiency of this method, it may potentially be applied on the scale of industrial production. At the same time, The Cu<sub>2</sub>O-CDs/NF/GCE also was applied to the detection of DA content in human serum with satisfactory results, and the biosensor could keep its activity for at least two months.

#### 5. Acknowledgments

This project was supported by the science and technology foundation of the national general administration of quality supervision in China (No. 2012QK053) and the education bureau of Fujian province of China (No. JB14180).

**References**

- [1] J. Deng, P. Yu, Y. Wang, L. Yang, L. Mao, *Adv. Mater.*, 2014, **26**, 6933-6943.
- [2] J. Song, J. Li, J. Xu, H. Zeng, *Nano letters*, 2014, **14**, 6298-6305.
- [3] J. Deng, P. Yu, Y. Wang, L. Mao, *Anal. Chem.*, 2015, **87**, 3080-3086.
- [4] C. Dong, R. Eldawud, L.M. Sargent, M.L. Kashaon, D. Lowry, Y. Rojanasakul, C.Z. Dinu, *Environ. Sci.: Nano*, 2014, **1**, 595-603.
- [5] J. Liu, S. Wagan, M. D. Morris, J. Taylor, R. J. White, *Anal. Chem.*, 2014, **86**, 11417-11424.
- [6] S.M. Majhi, P. Rai, S. Raj, B.S. Chon, K.K. Park, Y.T. Yu, *ACS Appl. Mater. Inter.*, 2014, **6**, 7491-7497.
- [7] G. Ghadimkhani, N. R. de Tacconi, W. Chanmanee, C. Janaky, K. Rajeshwar, *Chem. Commun.*, 2013, **49**, 1297-1299.
- [8] S. Ni, X. Lv, T. Li, X. Yang, L. Zhang, *Electrochim. Acta*, 2013, **109**, 419-425.
- [9] H. Li, X. Zhang, D.R. MacFarlane, *Adv. Energy Mater.*, 2015, **5**, 1401077.
- [10] F. Xu, M. Deng, G. Li, S. Chen, L. Wang, *Electrochim. Acta*, 2013, **88**, 59-65.
- [11] J. Liu, W. Zhu, S. Yu, X. Yan, *Carbon*, 2014, **79**, 369-379.
- [12] S.Y. Lim, W. Shen, Z. Gao, Carbon quantum dots and their applications, *Chem. Soc. Rev.*, 2015, **44**, 362.
- [13] X. Li, Y. Liu, X. Song, H. Wang, H. Gu, H. Zeng, *Angew. Chem. Int. Edit.*, 2015, **54**, 1759-1764.
- [14] C. Wei, Q. Huang, S. Hu, H. Zhang, W. Zhang, Z. Wang, M. Zhu, P. Dai, L. Huang, *Electrochim. Acta*, 2014, **149**, 237-244.
- [15] C.I. Wang, A.P. Periasamy, H.T. Chang, *Anal. Chem.*, 2013, **85**, 3263-3270.
- [16] Q. Huang, H. Zhang, S. Hu, F. Li, W. Weng, J. Chen, Q. Wang, Y. He, W. Zhang, X. Bao, *Biosens. Bioelectron.*, 2014, **52**, 277-280.
- [17] J. Yang, J.R. Strickler, S. Gunasekaran, *Nanoscale*, 2012, **4**, 4594-4602.
- [18] S. Zheng, Y. Huang, J. Cai, Y. Guo, *Int. J. Electrochem. Sci.*, 2013, **8**, 12296-12307.
- [19] A.C. Anithaa, N. Lavanya, K. Asokan, C. Sekar, *Electrochim. Acta*, 2015, **167**, 294-302.
- [20] S. Hu, Q. Huang, Y. Lin, C. Wei, H. Zhang, W. Zhang, Z. Guo, X. Bao, J. Shi, A. Hao, *Electrochim. Acta*, 2014, **130**, 805-809.

- [21] Y., P. Yu, L. Mao, *Analyst*, 2015, **140**, 3781-3787.
- [22] R. Devasenathipathy, V. Mani, S.M. Chen, B. Viswanath, V. S. Vasantha, M. Govindasamy, *RSC Adv.*, 2014, **4**, 55900-55907.
- [23] J. Liu, M.D. Morris, F.C. Macazo, L.R. Schoukroun-Barnes, R.J. White, *J. Electrochem. Soc.*, 2014, **161**, H301-H313.
- [24] P. Lu, J. Yu, Y. Lei, S. Lu, C. Wang, D. Liu, Q. Guo, *Sensor. Actuat. B: Chem.*, 2015, **208**, 90-98.
- [25] S. Yuan, W. Chen, S. Hu, *Mater. Sci. Eng. C*, 2005, **25**, 479-485.
- [26] B. Chen, F. Li, S. Li, W. Weng, H. Guo, T. Guo, X. Zhang, Y. Chen, T. Huang, X. Hong, S. You, Y. Lin, K. Zeng, S. Chen, *Nanoscale*, 2013, **5**, 1967-1971.
- [27] C.H. Kuo, C.H. Chen, M.H. Huang, *Adv. Funct. Mater.*, 2007, **17**, 3773-3780.
- [28] M. Bagherzadeh, M. Heydari, *Analyst*, 2013, **138**, 6044-6051.
- [29] E. Laviron, *J. Electroanal. Chem.*, 1979, **101**, 19-28.
- [30] Q. Huang, S. Hu, H. Zhang, J. Chen, Y. He, F. Li, W. Weng, J.Ni, X. Bao, Y. Lin, *Analyst*, 2013, **138**, 5417-5423.
- [31] S.K. Yadav, M. Oyama, R.N. Goyal, *J. Electrochem. Soc.*, 2014, **161**, H41-H46.
- [32] H. Bagheri, A. Afkhami, P. Hashemi, M. Ghanei, *RSC Adv.*, 2015, **5**, 21659-21669.
- [33] J. Sun, L. Li, X. Zhang, D. Liu, S. Lv, D. Zhu, T. Wu, T. You, *RSC Adv.*, 2015, **5**, 11925-11932.
- [34] G. Jiang, T. Jiang, H. Zhou, J. Yao, X. Kong, *RSC Adv.*, 2015, **5**, 9064-9068.
- [35] M. Lin, *RSC Adv.*, 2015, **5**, 9848-9851.
- [36] X. Fei, J. Luo, R. Liu, J. Liu, X. Liu, M. Chen, *RSC Adv.*, 2015, **5**, 18233-18241.
- [37] X. Feng, Y. Zhang, J. Zhou, Y. Li, S. Chen, L. Zhang, Y. Ma, L. Wang, X. Yan, *Nanoscale*, 2015, **7**, 2427-2432
- [38] Q. Lian, A. Luo, Z. An, Z. Li, Y. Guo, D. Zhang, Z. Xue, X. Zhou, X. Lu, *Appl. Surf. Sci.*, 2015, **349**, 184-189.
- [39] J. Salamon, Y. Sathishkumar, K. Ramachandran, Y.S. Lee, D.J. Yoo, A.R. Kim, G. Gnana kumara, *Biosens. Bioelectron.*, 2015, **64**, 269-276.
- [40] M. Rajamathi, J.S. Melo, T.V. Venkatesha, *Bioelectrochem.*, 2011, **81**, 104-108.

**Tables**

**Table 1** Comparison of the analytical performances on different modified electrodes.

**Table 2** Results of determination of DA in human serum (n = 5)

**Table 1** Comparison of the analytical performances on different modified electrodes.

Electrode	Linear range ( $\mu\text{M}$ )	Detection limit (nM)	References
$\text{Fe}_3\text{O}_4$ nanoparticle-decorated reduced graphene oxide	0.02-5.80	6.5	32
Nitrogen-doped carbon nanofiber	1.0-200	500	33
N-doped carbon quantum dots	0-1000	1.0	34
Gold nanoparticles/over-oxidized polypyrrole nanotube	0.025-2.5	10	35
Multiwalled carbon nanotubes/electroactive amphiphilic copolymer micelles	0.5-20, 200-1000	200	36
Three-dimensional nitrogen-doped graphene	3.0-100	1.0	37
gold nanoparticles/tryptophan-functionalized graphene nanocomposite	0.5-411	56	38
magnetite nanorods/graphene	0.01-100.55	7.0	39
$\text{WO}_3$ nanoparticles	0.1-600	24	19
$\text{Cu}_2\text{O}$ -CDs/NF	0.05-45.0	1.1	This work

**Table 2** Results of determination of DA in human serum (n = 5)

Human serum	Spiked ( $\mu\text{M}$ )	Found ( $\mu\text{M}$ )	Recovery (%)	RSD (%)
Sample 1	5.0	5.33	106.6	3.6
Sample 2	10.0	10.96	109.6	3.2
Sample 3	15.0	14.93	99.5	1.9
Sample 4	20.0	18.88	94.4	2.8
Sample 5	25.0	25.32	101.3	2.4

## Figures

**Fig. 1** (A) TEM image of CDs (B) SEM image of Cu<sub>2</sub>O-CDs, (C) the UV-vis spectra for CDs (a) and Cu<sub>2</sub>O-CDs composites (b), (D) XRD pattern for the obtained Cu<sub>2</sub>O-CDs.

**Fig. 2** 3D AFM images of bare GCE (A), NF/GCE (B), CDs/NF/GCE (C) and Cu<sub>2</sub>O-CDs/NF/GCE (D).

**Fig. 3** CVs of 0.1 mM DA recorded on bare GCE, NF/GCE, CDs/NF/GCE and Cu<sub>2</sub>O-CDs/NF/GCE in the pH 7.0 phosphate buffer solution (scan rate: 0.1 V s<sup>-1</sup>).

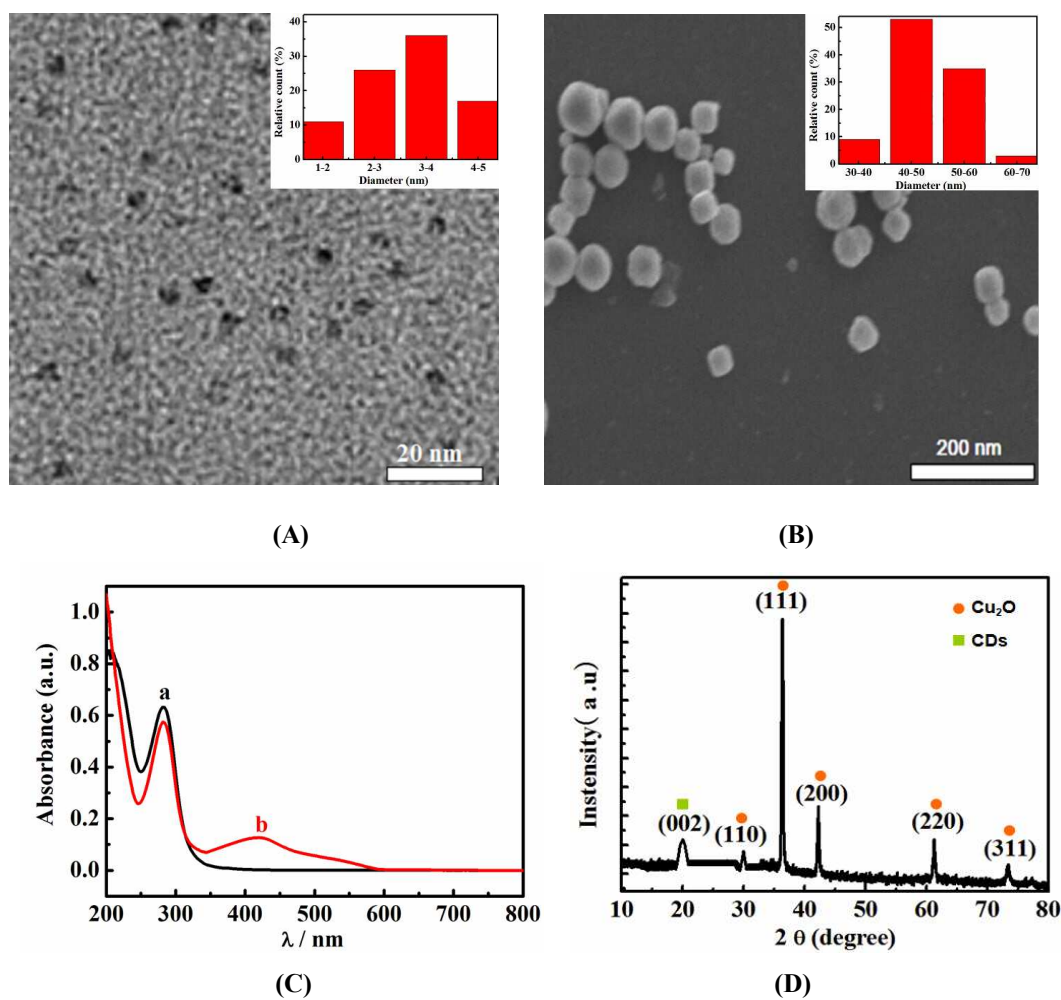
**Fig. 4** (A) The relationship of the  $E_{pa}$  and  $I_{pa}$  against pH (scan rate: 0.1 V s<sup>-1</sup>); (B) CV of 0.1 mM DA on Cu<sub>2</sub>O-CDs/NF/GCE in the pH 7.0 phosphate buffer solution at various scan rates (a-j: 0.05, 0.10, 0.15, 0.20, 0.25, 0.30, 0.35, 0.40, 0.45, 0.50 V s<sup>-1</sup>); (C) the relationships of  $I_{pa}$  and  $I_{pc}$  with  $v$  (D) the relationships of  $E_{pa}$  and  $E_{pc}$  with  $\log v$ .

**Fig. 5** The anode current peak (A) and zeta-potential (B) of 0.1 mM DA with the different concentrations of AA and UA: 0 mM (a), 10.0 mM (b), 50.0 mM (c) and 80.0 mM (d).

**Fig. 6** (A) DPVs of DA with increasing concentration (from a to l: 0.05, 1.0, 5.0, 10.0, 15.0, 20.0, 25.0, 30.0, 35.0, 40.0, 45.0  $\mu$ M). (B) The relationship of the  $I_{pa}$  with the concentration of DA.

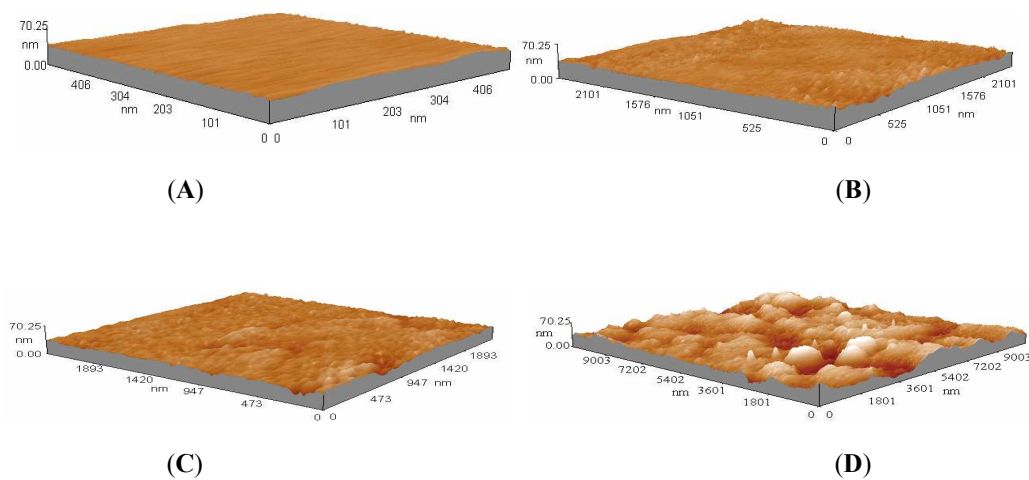


Fig. 1



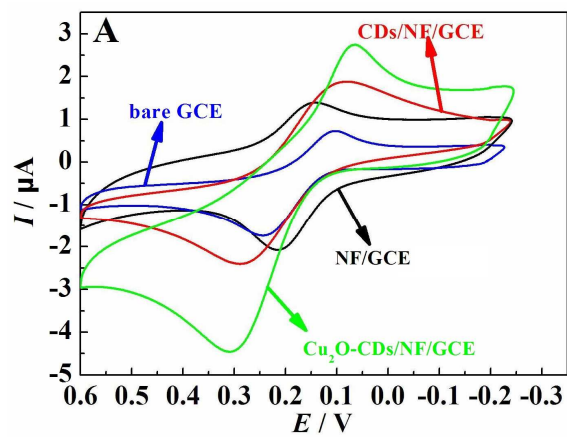
**Fig. 1** (A) TEM image of CDs (B) SEM image of Cu<sub>2</sub>O-CDs, (C) the UV-vis spectra for CDs (a) and Cu<sub>2</sub>O-CDs composites (b), (D) XRD pattern for the obtained Cu<sub>2</sub>O-CDs.

Fig. 2



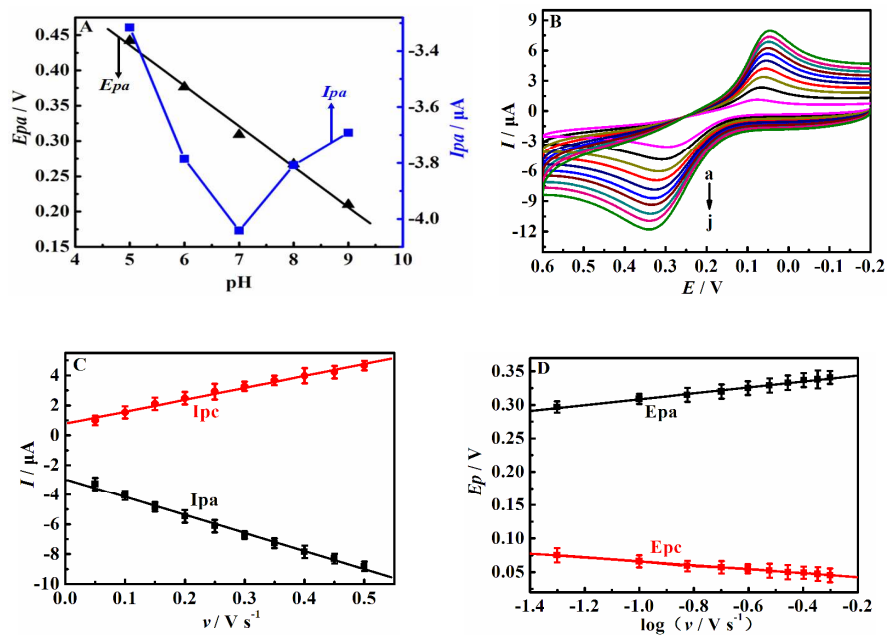
**Fig. 2** 3D AFM images of bare GCE (A), NF/GCE (B), CDs/NF/GCE (C) and  $\text{Cu}_2\text{O}$ -CDs/NF/GCE (D).

Fig. 3



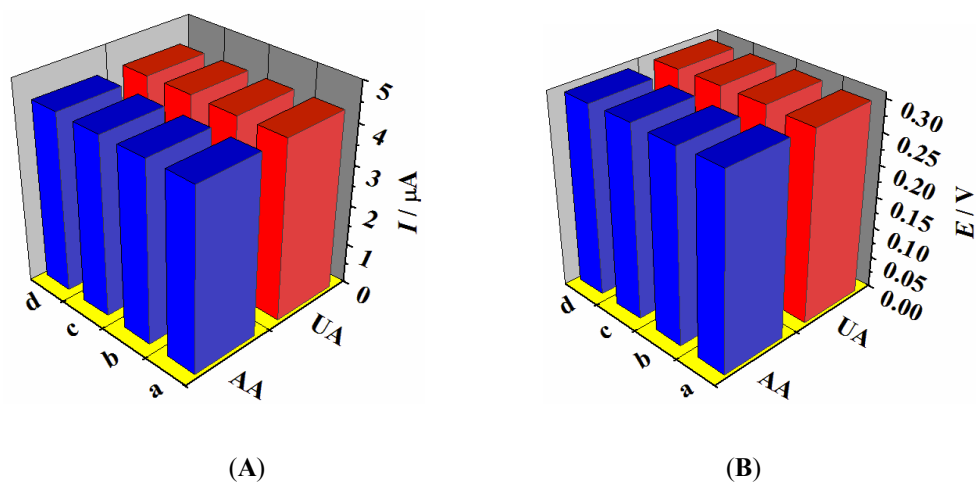
**Fig. 3** CVs of 0.1 mM DA recorded on bare GCE, NF/GCE, CDs/NF/GCE and Cu<sub>2</sub>O-CDs/NF/GCE in the pH 7.0 phosphate buffer solution (scan rate: 0.1 V s<sup>-1</sup>).

Fig. 4



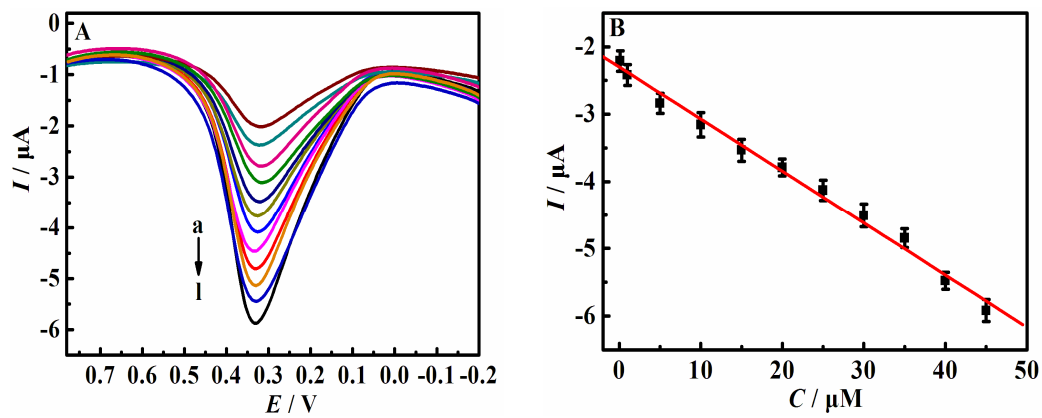
**Fig. 4** (A) The relationship of the  $E_{pa}$  and  $I_{pa}$  against pH (scan rate:  $0.1 V s^{-1}$ ); (B) CV of 0.1 mM DA on Cu<sub>2</sub>O-CDs/NF/GCE in the pH 7.0 phosphate buffer solution at various scan rates (a-j: 0.05, 0.10, 0.15, 0.20, 0.25, 0.30, 0.35, 0.40, 0.45, 0.50  $V s^{-1}$ ); (C) the relationships of  $I_{pa}$  and  $I_{pc}$  with  $v$  (D) the relationships of  $E_{pa}$  and  $E_{pc}$  with  $\log v$ .

Fig. 5



**Fig. 5** The anode current peak (A) and zeta-potential (B) of 0.1 mM DA with the different concentrations of AA and UA: 0 mM (a), 10.0 mM (b), 50.0 mM (c) and 80.0 mM (d).

Fig. 6



**Fig. 6 (A)** DPVs of DA with increasing concentration (from a to l: 0.05, 1.0, 5.0, 10.0, 15.0, 20.0, 25.0, 30.0, 35.0, 40.0, 45.0  $\mu\text{M}$ ). **(B)** The relationship of the  $I_{pa}$  with the concentration of DA.